2023 45th Annual International Conference of the IEEE Engineering in Medicine & Biology Society (EMBC) | 979-8-3503-2447-1/23/$31.00 ©2023 IEEE | DOI: 10.1109/EMBC40787.2023.10340677

Eight-channel SiNx microring-resonator based photonic biosensor for label-free fluid analysis in the optical C-band*

Jakob Reck[1], Moritz Kleinert[1], Klara Mihov[1], Martin Kresse[1], Cafercan Yilmaz[1], Christina Hoffmann[2], Peter Hoffmann[2], Vera Froese[3], Ulrich Kertzscher[3], Kristina Mykhailiuk[5], Julia Michaelis[5], Wilfried Weigel[5], Sören Scholand[6], Hans-Jürgen Heupke[6], Madeleine Weigel[1], David de Felipe[1], Tianwen Qian[1], Hauke Conradi[1], Crispin Zawadzki[1], Norbert Keil[1], Martin Schell[1,4]

***Abstract*— A lab-on-a-chip multichannel sensing platform for biomedical analysis based on optical silicon nitride (SiNx) microring-resonators (MRR) was established. The resonators were surface functionalized and finally combined with a microfluidic chamber for validation using an avidin-biotin ligand-binding assay. The results with a limit of detection (*LOD*) of $2.3 \cdot 10^{-5}$ and a mean intra-assay coefficient of variation (*CV*) of ±10.0 %, also under consideration of FDA guidelines, show promising future applicability for a wide variety of targets in the field of outpatient medical diagnostics and life science.**

***Clinical Relevance*— Biomarkers play a crucial role in physiological processes of the human body. To enable instantaneous and decentralized analysis of these markers, systems are needed that can be used in a laboratory-independent environment with minimal amounts of biofluid. An example is the utilization of such systems for neonates or infants.**

I. Introduction

Silicon nitride-based photonic integrated circuits (PICs) are gaining significant importance not only in optical communication and quantum applications, but also in optical sensing [1]. Due to extremely high integration capability and sensitivity paired with a very rapid data analysis, an application in the context of biomedical sensing is evident. This paper presents research done to establish an eight-channel photonic sensor chip based on silicon nitride (SiNx) microring-resonators (MRR) to enable a disposable lab-on-a-chip waveguide platform working in the optical C-band with a base wavelength at about 1550 nm. Cost efficiency is achieved by basing the value chain on CMOS compatible PIC technology. This includes, for example, wafer-scale manufacturing and functionalization combined with passive pick-and-place processing. Target is to analyze very low sample volumes, e.g. for the detection of bioindicators or pathogens, which is of immense importance for *in vitro* medical diagnostics and therapy monitoring [2]. This multi-channel approach can be used to implement quantitative and qualitative multi-parameter measurement.

In the study, the aim was to functionalize the MRR surface with capture molecules to validate the label-free surface-sensing sensor [3] with a receptor-ligand binding assay (LBA). With the use of appropriate microfluidics, the sample volume flow can be controlled accordingly so that the reaction kinetics are made detectable as the selected biomarkers bind to the active-surface elements. The detection principle is based on the change of the effective refractive index in the waveguide through the coupling of its evanescent field with the environment. This leads to a resonance wavelength shift of the MRR. The change in the optical properties and the output wave signal indicate a proportional interaction to the amount of particles attached [4]. In this work, both the quality factor Q and the *LOD* should be improved in a multi-channel setting in comparison to other similar studies. Additionally, a proper *CV* should be demonstrated.

II. Theoretical Analysis

Optical microring-resonators have been researched for years in various configurations such as optical networks, filters, sensors and buffers [5]. The notch filter configuration used here blocks a single wavelength in the transmission path. It consists of a single-mode straight waveguide and a MRR, a so-called racetrack resonator (Fig. 1a). The term racetrack resonator stems from a straight coupling region in the form of a multi-mode interference coupler (MMI) [6], resembling an oval track in a car race.

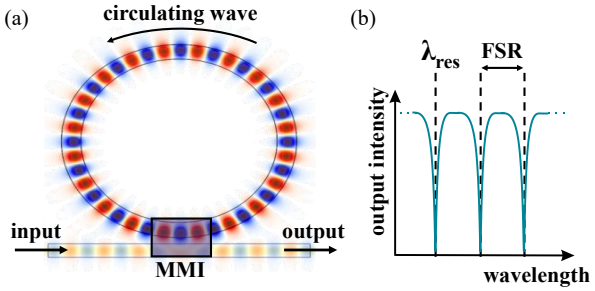

Figure 1. Schematic illustration of the optical resonant cavity concept with bus waveguide, MMI and MRR (a). Resulting resonance characteristics of the system with typical wavelength dependent dips are illustrated in (b).

After coupling into the cavity, optical interference occurs between the circulating waveguide mode and the input mode through the MMI. With the effective refractive index n_{eff}, the resonator radius at waveguide center r and an integer m, the

*Research co-funded by the German Federal Ministry of Education and Research within the framework of KMU-innovativ (ID: 13GW0243B)

[1] Fraunhofer Institute for Telecommunications, Heinrich Hertz Institute, HHI, Photonic Components Department, Berlin, Germany
[2] Charité – Universitätsmedizin Berlin, Institute of Diagnostic Laboratory Medicine, Clinical Chemistry and Pathobiochemistry, Berlin, Germany
[3] Charité – Universitätsmedizin Berlin, Institute of Computer-assisted Cardiovascular Medicine, Biofluid Mechanics Laboratory, Berlin, Germany
[4] Technische Universität Berlin, Berlin, Germany
[5] SCIENION GmbH, Berlin, Germany
[6] ESCHWEILER GmbH & CO.KG, Kiel, Germany

resonance wavelengths λ_{res} can be calculated by (1) [5]. Consequently, the position of the resonance peaks correlates with the refractive index *RI* near the waveguide core and can be monitored by using a tunable laser source for scanning the desired wavelength range. A proper resonance characteristic is crucial for the subsequent algorithms for detection and evaluation of the resonance wavelength shift (Fig 1b).

$$\lambda_{res} = (2\pi r \cdot n_{eff}) / m \qquad (1)$$

The factor *Q* according to (2) describes the wavelength selectivity and is calculated by dividing the free spectral range (*FSR*) by the corresponding full width at half maximum (*FWHM*). Accordingly, small *FWHM* cause large Q-factors and thus enable more precise identification of resonance wavelengths.

$$Q = \lambda_{res} / FWHM_{\lambda_{res}} \qquad (2)$$

For PIC-powered biosensing applications a suitable characteristic is the bulk sensitivity S_B (3), which is defined by the shift of the resonance wavelength $\Delta\lambda_{res}$ as a function of the change in the refractive index Δn [7]. This sensitivity can be determined metrological from the increase in resonance wavelength shift via the refractive index change.

$$S_B = \frac{(\lambda / n_{eff2}) - (\lambda / n_{eff1})}{\Delta n} = \frac{\Delta\lambda_{res}}{\Delta n} \qquad (3)$$

$$limit\ of\ detection\ (LOD) = \frac{Resolution\ (R)}{Sensitivity\ (S_B)} \qquad (4)$$

The decisive criterion for a high-resolution and precise sensor is the limit of detection (*LOD*), which combines resolution *R* and sensitivity S_B with (4). It describes the smallest detectable refractive index change and is suitable as a measure for comparing refractive index based sensor systems [8].

III. Design and Fabrication

For the photonic sensor system, the aim was to enable not only a compact design but also simple handling for the user. A system was developed that separates the optoelectronic components and the SiNx PIC (Fig. 2). This allows the sensor chip to be replaced after a certain number of measurements without having to make further adjustments to the overall system.

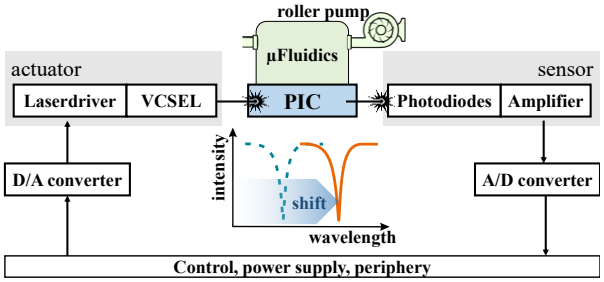

Figure 2. Sensor optoelectronic signal chain for real-time measurement. Refractive index change at the waveguide surface leads to a resonance wavelength shift.

Reason for choosing the optical C-band is to create a system with high eye safety by using good available optical components from the telecommunications market.

A. SiNx Photonic Sensorchip

To ensure efficient signal interaction between waveguide core and analyte, the waveguides are designed as low confinement structures so that the evanescent field radiates as far as possible into the measurement environment without showing significant losses. Fig. 3 shows the CAD layout of the biosensor chip with waveguides, polarization-dependent MMIs for light distribution (three-stage cascade of MMIs) and MRRs as operating sensor elements. High tolerant grating couplers enable optic coupling to the single-mode waveguides on the PIC. These periodic structures deflect the light at a specific angle out of the plane of the sensor chip, allowing non-contact optical coupling [9]. This coupling method enables a fully passive alignment [10]. Details will be described elsewhere.

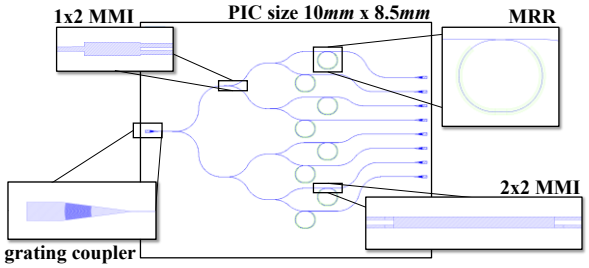

Figure 3. PIC architecture with detailed view of the photonic building blocks such as grating couplers, MMIs and MRR.

The CAD layout of the sensor chip was taken for the manufacturing of a lithographic mask. Subsequently, the optical sensors were fabricated on 4-inch wafers using CMOS (complementary metal-oxide-semiconductor) compatible PIC technology. In order to ensure single-mode operation at a 1550 *nm* wavelength, an area for a 150 *nm* by 1500 *nm* waveguide cross section, a basic layer stack (top to bottom) of 420 *nm* silicon dioxide (SiO_2), 200 *nm* silicon nitride (Si_3N_4) and 3.4 *µm* thermal SiO_2 on 525 *µm* silicon (Si) substrate was used. To be able to attach the appropriate molecular linkers near the waveguide core, it was necessary to expose the waveguide locally around the MRR by a lift-off process in the last step [11]. In the PIC manufacturing process, a yield of over 95 % was achieved.

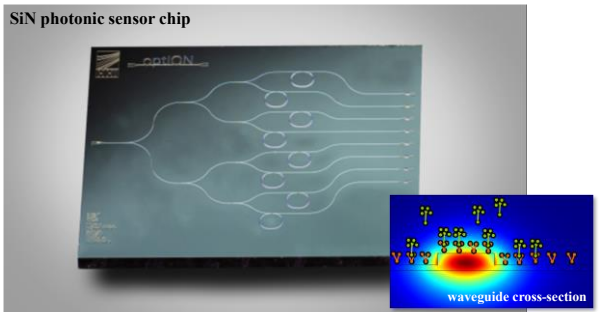

Figure 4. Manufactured PIC (size 10 *mm* x 8.5 *mm*) with eight channels for biomedical fluid analysis and schematic view of the binding of scavenger molecules in cross-section view.

The resulting multichannel photonic chips have a size of 10 *mm* x 8.5 *mm* each after wafer dicing separation (Fig. 4).

B. Surface Functionalization

To be able to analyze target molecules, the sensor's surface was first functionalized with appropriate capture molecules.

For validation, a biotin-neutravidin binding was chosen as a model system, known to form the strongest non-covalent bond in biochemistry [12]. Therefore, biotin-BSA, a biotin-labeled protein widely used in bioanalytics, was selected as capture molecule for the target neutravidin. To remove organic residues from the SiNx PIC and to generate a sufficient number of hydroxy groups on its surface, the sensors were exposed to oxygen plasma. In the next step, the chips were functionalized with an amino silane followed by modification with glutaraldehyde. For the precise deposition of capture molecules, Scienion's sciFLEXARRAYER pico technology was used. With the non-contact dispensing device, 120 *nL* biotin-BSA (10 *µg/mL* biotin-BSA in 1 *M* phosphate buffer) were deposited onto six chosen MRR structures. The remaining MRRs were used as reference structures onto which 48 *nL* BSA (10 *µg/mL* BSA in 1 *M* phosphate buffer) were deposited. Additionally, they are used in data evaluation to rule out influences such as temperature fluctuations or global artifacts. Focus of the research was to ensure that the biofunctionalization is suitable for measurements in the described system and that reproducible results can be achieved.

After the deposition, the functionalized chips were incubated at 75 *%* relative humidity overnight to allow the reaction between the proteins and the glutaraldehyde on the surface. A subsequent blocking step prevents nonspecific bindings of analytes during the measurements. The utilization of the sciFLEXARRAYER technology for biofunctionalization allows for the realization of versatile applications. With this approach, each MRR could be equipped with a different capture molecule to perform multiplex-assays with just one sample in future applications. This is not possible with standard bulk incubation.

C. Microfluidics

To ensure controlled analyte flow to the parallel microring-resonators, a 3D-printed micro chamber from polymer material was designed as an interface between chemical media and physical-optical sensor. Uniform MRR overflow is important to evaluate real-time interaction on the open waveguide surface.

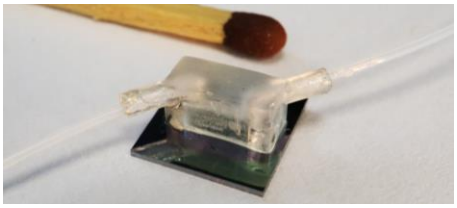

Figure 5. Combination of photonic sensor chip with 3D-printed microfluidics (volume < 50 *µl*) for delivery of an analyte.

The microfluidics (Fig. 5) provide a volume of < 50 *µL* and can be applied directly onto the chip as a replaceable component.

IV. Characterization

The characterization of the developed system provides information both about the optical parameters and about the usability as a biosensor. The latter also in comparison with the specifications considering the coefficient of variation (*CV*, (5)) from the bioanalytical method validation guidance for industry published by the U.S. Food and Drug Administration (FDA) as benchmark [13]. A validation recommendation of *CV* < ±20.0 *%* is specified therein for LBAs.

$$CV = \frac{standard\ deviation\ (data)}{mean\ (data)} \qquad (5)$$

A. Optical Characterization

Optical characterization of modulation depths and *Q*-factors was investigated on non-functionalized PICs. A benchtop C-band tunable laser was used to couple transverse-electrical polarized light into the PIC via lensed optical fibers. On the side of the sensor, a component tester detected signals after passing through the chip. Fig. 6 shows typical data with clearly identifiable modulation depths greater than 10 *dB* and an observed standard deviation of the signal intensity with less than 0.2 *dB*, which is more than sufficient for the overall system. A *Q*-factor of $1.2 \cdot 10^5$ is achieved. In comparison to similar studies reviewed in [14], [15] and [16], maximum *Q*-factors of $7.0 \cdot 10^4$ were achieved.

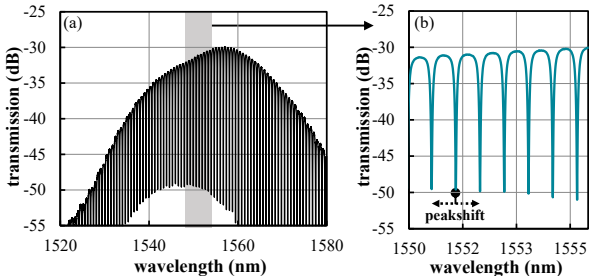

Figure 6. Typical transmission spectra of the optical microring-resonator with modulation depth in (a) and (b).

To estimate the resolution and sensitivity of the sensors, the PIC was integrated with the developed microfluidics. The response to the environmental changes was measured by exposing alternating sodium chloride (NaCl) solutions of increasing concentration (doubled after each cycle) and distilled water to the sensor. It can be seen clearly that e.g. a doubling of the NaCl concentration results in a doubling of the change in the resonance wavelength (Fig. 6). The evaluated data in Fig 7 show a linear correlation fitting with a sensitivity of 128 *nm/RIU*. This agrees well with the value of 139 *nm/RIU* determined numerically in the system design phase.

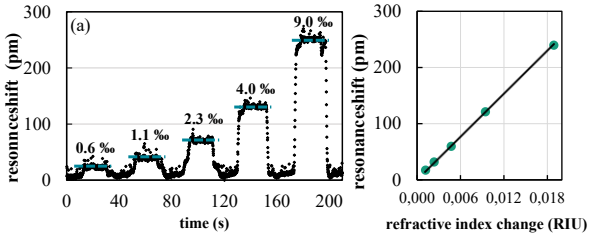

Figure 7. The response of the system to environmental changes around the waveguide core shown by resonance peak shift (a). Different NaCl concentrations were used to demonstrate linear relationship (b) between refractive index change and resonance peak shift ($R^2 = 0.997$).

The measurement signal taken with a sampling rate of 10 *sps* shows a standard deviation *SD* of 3.0 *pm*. According to (4) this results in a system *LOD* of $2.3 \cdot 10^{-5}$. On-chip systems with similar microring–resonator based configurations [14, 15, 16, 17, 18] presented a system *LOD* in the

range of $10^{-4} \sim 10^{-6}$. The results of this work are thus comparable.

B. Volumetric Sensing with Functionalized Sensor

In addition to the initial optical characterization, the multichannel experiments for the detection of neutravidin on biotin-BSA functionalized SiNx microring-resonators were demonstrated. For this purpose, the functionalized PICs were integrated in the measurement system described in Fig. 2.

To generate a baseline for further measurement of the analyte sample, the photonic sensor chips were first flushed with a 1x PBS solution. PBS is widely used for these kinds of biomedical applications because it provides the osmotic pressure and ion concentration of the human bio system [19]. Subsequently, either 50 *µg/ml* or 10 *µg/ml* neutravidin in 1x PBS solutions were introduced. Finally, a washing step with a 0.5 *%* Tween 20 in 1x PBS solution followed by 1x PBS was performed in the same measuring cycle. A selection of the measured time series is shown in Fig. 8. It was expected that the reference channels, which were only biofunctionalized with BSA, should give significantly lower response after reaction with neutravidin compared to biotin-BSA biofunctionalized structures. This was verified by the experimental results which indicates that the biofunctionalization of the microring-resonators structures was successful and is suitable for future assay application.

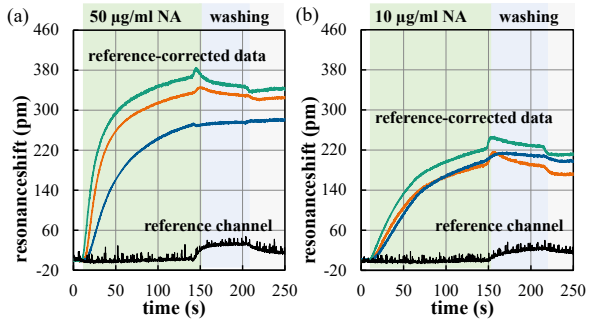

Figure 8. Measurement series with 50 µg/ml neutravidin concentration (a) and 10 µg/ml neutravidin concentration (b).

In order to analyze the difference of spread in the data, all relative to the mean value, the CV was calculated for two different analyte concentrations.

Data for 50 *µg/ml* neutravidin show an intra-assay *mean(CV)* of ±10.0 *%* (*SD* = 4.2). The data for 10 *µg/ml* neutravidin result in *mean(CV)* = ±13.9 *%* (*SD* = 7.8). From an inter-assay point of view, *CV* is ±13.9 *%* for 50 *µg/ml* and ±11.0 *%* for 10 *µg/ml* neutravidin. In comparison to the FDA validation recommendation (*CV* < ±20.0 *%*), it can be stated that the developed MRR based system remains well below this threshold. The use of the sensor system under dynamic changes of the environment by applying sample fluids could thus be successfully demonstrated.

V. Conclusion

In this study, an interdisciplinary approach was taken to develop a miniaturized sensor system based on SiNx PIC technology. The results indicate a good applicability of photonic SiNx MRRs as biosensors in highly integrable, portable, multichannel and real-time point-of-care devices for medical diagnostics. Compared to similar studies, the presented functionalized PIC shows a high *Q*-factor with a good comparable *LOD* at the same time. A special feature is the precise deposition of different capture molecules on a single chip. Applications such as life science, environmental analytics and food analysis will be investigated in future work with typical target groups such as proteins, small molecules, vitamins, viruses, bacteria or nucleic acids.

References

[1] M. Schell et al., "Hybrid photonic integration for communication, sensing and quantum technology," in Integrated Optics: Devices, Materials, and Technologies XXVI, 2022.

[2] W. B. Mattes and F. Goodsaid, "Regulatory landscapes for biomarkers and diagnostic tests: Qualification, approval, and role in clinical practice," Exp. Biol. Med. (Maywood), vol. 243, no. 3, pp. 256–261, 2018.

[3] C. Ciminelli, C. M. Campanella, F. Dell'Olio, C. E. Campanella, and M. N. Armenise, "Label-free optical resonant sensors for biochemical applications," Prog. Quantum Electron., vol. 37, no. 2, pp. 51–107, 2013.

[4] A. L. Washburn and R. C. Bailey, "Photonics-on-a-chip: recent advances in integrated waveguides as enabling detection elements for real-world, lab-on-a-chip biosensing applications," Analyst, vol. 136, no. 2, pp. 227–236, 2011.

[5] W. Bogaerts et al., "Silicon microring resonators," Laser Photon. Rev., vol. 6, no. 1, pp. 47–73, 2012.

[6] A. Kaźmierczak, "Light coupling and distribution for Si3N4/SiO2 integrated multichannel single-mode sensing system," Opt. Eng., vol. 48, no. 1, p. 014401, 2009.

[7] L. Chrostowski et al., "Silicon photonic resonator sensors and devices." Society of Photo-Optical Instrumentation Engineers (SPIE), 2012.

[8] Í. Molina-Fernández, J. Leuermann, A. Ortega-Moñux, J. G. Wangüemert-Pérez, and R. Halir, "Fundamental limit of detection of photonic biosensors with coherent phase read-out," Opt. Express, vol. 27, no. 9, pp. 12616–12629, 2019.

[9] C. R. Doerr, L. Chen, Y.-K. Chen, and L. L. Buhl, "Wide bandwidth silicon nitride grating coupler," IEEE Photonics Technol. Lett., vol. 22, no. 19, pp. 1461–1463, 2010.

[10] Fraunhofer HHI. "Photonics for Point-of-Care Sensor Systems - Fiber optic coupling of high-precision disposables" YouTube, Mar. 28, 2022 [Video file]. Available: https://youtu.be/xovf23Y-WLI. [Accessed: Apr. 27, 2023].

[11] C. Schulte-Osseili, M. Kleinert, N. Keil, and R. R. Rosencrantz, "Rapid drop-test for lectin binding with glycopolymer-coated optical ring resonators," Biosensors (Basel), vol. 9, no. 1, p. 24, 2019.

[12] A. Jain and K. Cheng, "The principles and applications of avidin-based nanoparticles in drug delivery and diagnosis," J. Control. Release, vol. 245, pp. 27–40, 2017.

[13] Food and Drug Administration, „Bioanalytical Method Validation Guidance for Industry", Silver Spring, 2018.

[14] D. Rho, C. Breaux, and S. Kim, "Label-free optical resonator-based biosensors," Sensors (Basel), vol. 20, no. 20, p. 5901, 2020.

[15] E. Luan, H. Shoman, D. M. Ratner, K. C. Cheung, and L. Chrostowski, "Silicon photonic biosensors using label-free detection," Sensors (Basel), vol. 18, no. 10, p. 3519, 2018.

[16] B. Shi, X. Chen, Y. Cai, S. Zhang, T. Wang, and Y. Wang, "Compact slot microring resonator for sensitive and label-free optical sensing," Sensors (Basel), vol. 22, no. 17, p. 6467, 2022.

[17] A. Jain and K. Cheng, "The principles and applications of avidin-based nanoparticles in drug delivery and diagnosis," J. Control. Release, vol. 245, pp. 27–40, 2017.

[18] N. Mudgal, A. Agarwal, A. Saharia, S. Sahu, A. K. Ghunawat, and G. Singh, "Comparative study of interferometer and ring resonator based biosensors: A review," in Lecture Notes in Electrical Engineering, Singapore: Springer Singapore, 2020, pp. 419–427.

[19] N. I. Khan and E. Song, "Lab-on-a-chip systems for aptamer-based biosensing," Micromachines (Basel), vol. 11, no. 2, p. 220, 2020.